





Article

Maletoyvayamite, $\text{Au}_3\text{Se}_4\text{Te}_6$, a new mineral from Maletoyvayam deposit, Kamchatka peninsula, Russia

Nadhezda D. Tolstykh^{1,2}, Marek Tuhý^{3,4*} , Anna Vymazalová³ , Jakub Plášil⁵, František Laufek³, Anatoly V. Kasatkin⁶, Fabrizio Nestola⁷ and Olga V. Bobrova⁸

¹VS Sobolev Institute of Geology and Mineralogy, SB RAS, prosp. Akademika Koptuyga 3, 630090, Novosibirsk, Russia; ²Novosibirsk State University, Pirogova street 1, Novosibirsk, 630090, Russia; ³Czech Geological Survey, Geologická 6, 152 00 Prague 5, Czech Republic; ⁴Institute of Mineralogy, Geochemistry and Mineral Resources, Faculty of Science, Charles University, Albertov 6, 128 00 Prague 2, Czech Republic; ⁵Institute of Physics ASCR, v.v.i., Na Slovance 2, 128 21 Prague 8, Czech Republic; ⁶Fersman Mineralogical Museum of Russian Academy of Sciences, Leninsky Prospekt 18-2, 119071 Moscow, Russia; ⁷Dipartimento di Geoscienze, Università di Padova, Via Gradenigo 6, I-35131, Padova, Italy; and ⁸StekloSoyuz, Dept of raw materials, Zhuravleva 2, Moscow 107023, Russia

Abstract

Maletoyvayamite, $\text{Au}_3\text{Se}_4\text{Te}_6$, is a new mineral discovered in a heavy-mineral concentrate from the Gaching occurrence of the Maletoyvayam deposit, Kamchatka, Russia (60°19'51.87"N, 164°46'25.65"E). It forms anhedral grains (10 to 50 μm in size) and is found in intergrowths with native gold (Au–Ag), Au tellurides (calaverite), unnamed phases (AuSe, Au_2TeSe and Au oxide), native tellurium, sulfosalts (tennantite, tetrahedrite, goldfieldite and watanabeite) and supergene tripuhite. Maletoyvayamite has a good cleavage on {010} and {001}. In plane-polarised light, maletoyvayamite is grey, has strong bireflectance (grey to bluish grey), and strong anisotropy; it exhibits no internal reflections. Reflectance values for maletoyvayamite in air (R_{min} , R_{max} in %) are: 38.9, 39.1 at 470 nm; 39.3, 39.5 at 546 nm; 39.3, 39.6 at 589 nm; and 39.4, 39.7 at 650 nm. Sixteen electron-microprobe analyses of maletoyvayamite gave an average composition: Au 34.46, Se 16.76, Te 47.23 and S 0.84, total 99.29 wt.%, corresponding to the formula $\text{Au}_{2.90}(\text{Se}_{3.52}\text{S}_{0.44})_{\Sigma 3.96}\text{Te}_{6.14}$ based on 13 atoms; the average of eleven analyses on synthetic analogue is: Au 34.20, Se 19.68 and Te 45.42, total 99.30 wt.%, corresponding to $\text{Au}_{2.90}\text{Se}_{4.16}\text{Te}_{5.94}$. The calculated density is 7.98 g/cm^3 . The mineral is triclinic, space group $P\bar{1}$, with $a = 8.901(2)$, $b = 9.0451(14)$, $c = 9.265(4)$ Å, $\alpha = 97.66(3)$, $\beta = 106.70(2)$, $\gamma = 101.399(14)^\circ$, $V = 685.9(4)$ Å³ and $Z = 2$. The crystal structure of maletoyvayamite represents a unique structure type resembling a molecular structure. There are cube-like $[\text{Au}_6\text{Se}_8\text{Te}_{12}]$ clusters linked *via* van der Waals interactions. The structural identity of maletoyvayamite with the synthetic $\text{Au}_3\text{Se}_4\text{Te}_6$ was confirmed by powder X-ray diffraction and Raman spectroscopy.

Keywords: maletoyvayamite, $\text{Au}_3\text{Se}_4\text{Te}_6$, reflectance, chemical composition, X-ray diffraction, crystal structure, Gaching Au mineralisation, Maletoyvayam deposit, Kamchatka, Russia

(Received 16 October 2019; accepted 14 December 2019; Accepted Manuscript published online: 21 January 2020;
Associate Editor: Juraj Majzlan)

Introduction

The polished section that contains grains of maletoyvayamite [pronounced: ma-le-toy-va-ya-mite], ideally $\text{Au}_3\text{Se}_4\text{Te}_6$, comes from the Gaching occurrence of the Maletoyvayam deposit located in the southwestern part of the Koryak Highland of the central Kamchatka volcanic belt, Far East, Russia (60°19'51.87"N, 164°46'25.65"E). The Gaching Au mineralisation in the Maletoyvayam deposit is located in the Eocene–Oligocene central Kamchatka volcanic belt ~1800 km long (Fig. 1). The latter includes a number of other gold–silver epithermal deposits: Ozernovskoe, Aginskoe and Asachi (Goryachev *et al.*, 2010). The Maletoyvayam deposit is composed of andesites, tuffs and tuffaceous sandstones (Melkomukov *et al.*, 2010). The main gangue minerals

are quartz, alunite, native sulfur and kaolinite. On the basis of the typomorphic features of mineral assemblages, the Maletoyvayam deposit belongs to high-sulfidation (HS type) epithermal deposits (Okrugin 2003; Okrugin *et al.*, 2014; Kalinin *et al.*, 2012).

The vein and disseminated mineralisation in the Maletoyvayam deposit include pyrite, native gold and Au tellurides/selenides in association with Cu sulfosalts in quartzites and quartz–alunite altered rocks. Maletoyvayamite was described originally as an unnamed phase with the composition $\text{Au}_2(\text{Se,S})_3\text{Te}_4$ (Tolstykh *et al.*, 2017, 2018). It was noted that such a compound has never been found before in any other epithermal deposit.

Both the mineral and its name were approved by the Commission on New Minerals, Nomenclature and Classification of the International Mineralogical Association (IMA2019-021, Tolstykh *et al.*, 2019b). The name maletoyvayamite (Cyrillic – малотойваямит) is after its type locality, the Maletoyvayam deposit in the Kamchatka peninsula, Russia.

Holotype material with maletoyvayamite (polished section) along with its synthetic analogue (Exp Au2) are deposited in

*Author for correspondence: Marek Tuhý, Email: marek.tuhý@geology.cz

Cite this article: Tolstykh N.D., Tuhý M., Vymazalová A., Plášil J., Laufek F., Kasatkin A.V., Nestola F. and Bobrova O.V. (2020) Maletoyvayamite, $\text{Au}_3\text{Se}_4\text{Te}_6$, a new mineral from Maletoyvayam deposit, Kamchatka peninsula, Russia. *Mineralogical Magazine* 84, 117–123. <https://doi.org/10.1180/mgm.2019.81>

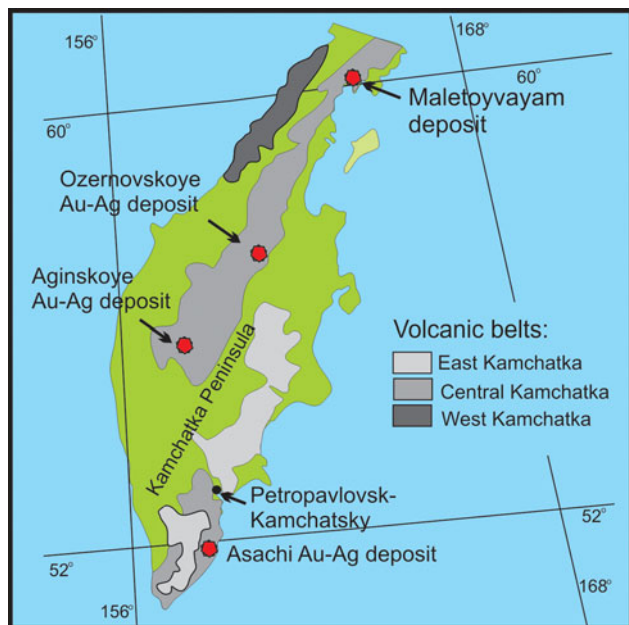


Fig. 1. Volcanic belts of the Kamchatka Peninsula (adapted from Tsukanov, 2015), and location of the epithermal deposits.

the Central Siberian Geological Museum (CSGM) of VS Sobolev Institute of Geology and Mineralogy of Siberian Branch of the Russian Academy of Sciences (SB RAS), Novosibirsk, Russia, catalogue number V-9/1.

Appearance, physical and optical properties

The individual grains (10–50 μm) of maletoyvayamite in intergrowths with native gold, calaverite, unnamed phases of AuSe–AuTe and Te–Se solid solutions, and sulfosalts (tennantite–tetrahedrite, goldfieldite, watanabeite) were found in a heavy-mineral concentrate. Associated minerals are ‘mustard gold’, complex Au oxides [(Au,Ag)–(Sb,As,Te,S)–O], senarmontite, tripuhyite, rooseveltite, tiemannite, antimonselite and guanajuatite. Associated calaverite has been oxidised in hypergenic conditions into mustard gold mixed with the Fe–Sb oxides (tripuhyite) and goethite or transformed into Au–Sb(Te,Se,S,As) oxides, whereas maletoyvayamite is stable in this environment and not oxidised (Tolstykh *et al.*, 2019a). Back-scattered electron images of maletoyvayamite and associated minerals are shown in Fig. 2. Maletoyvayamite is opaque with metallic lustre. Cleavage is good on {010} and {001}, parting not observed. The powder of the synthetic analogue is grey in colour and has a grey streak. The mineral is brittle. The density calculated on the base of the empirical formula is 7.967 g cm^{-3} . In plane-polarised reflected light maletoyvayamite is bluish grey, has strong birefractance, strong anisotropy and exhibits no internal reflections. Reflectance was measured in air relative to a WTiC standard using a Zeiss 370 spectrophotometer MSP400 TIDAS mounted to Leica microscope with a 50 \times objective (National Museum in Prague, Czech Republic). Data are given in Table 1 and plotted in Fig. 3.

Synthetic analogue

Single-crystal X-ray studies of (natural) maletoyvayamite could not be carried out because the crystals tested were too poor.

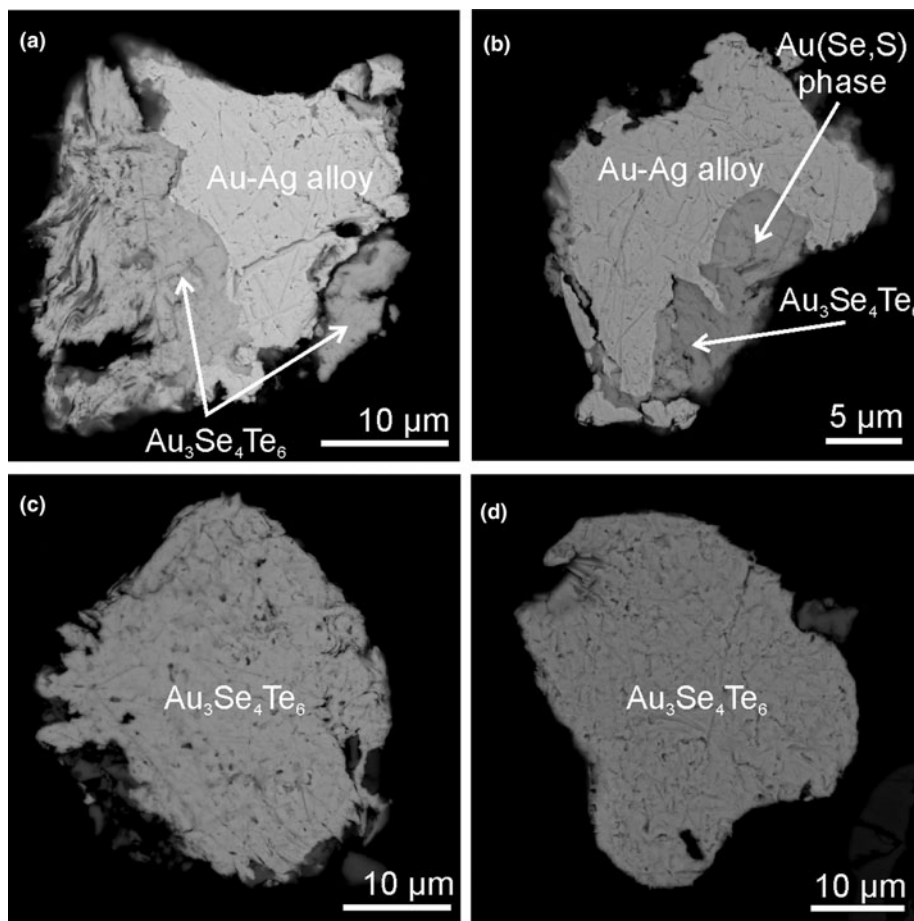
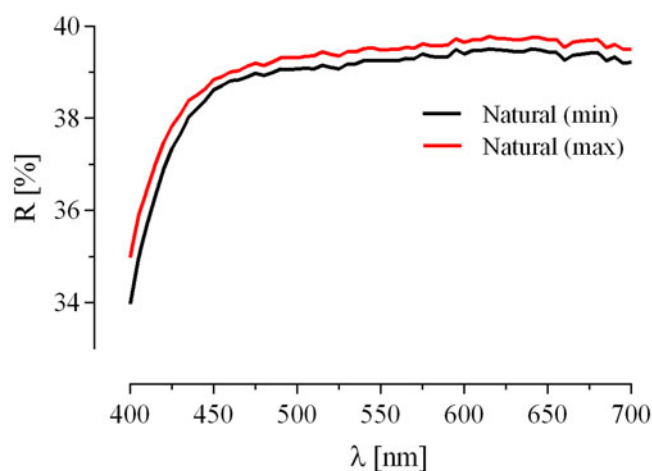


Fig. 2. Back-scattered electron micrographs (FEGSEM) of maletoyvayamite ($\text{Au}_3\text{Se}_4\text{Te}_6$) intergrown with (a) Au–Ag alloy, (b) Au–Ag alloy and unidentified Au (Se,S) phase and (c,d) individual maletoyvayamite grains which were used for Raman spectroscopy analyses.

Table 1. Reflectance data of maletoyvayamite.

λ (nm)	R_{\min} (%)	R_{\max} (%)	λ (nm)	R_{\min} (%)	R_{\max} (%)
400	34.0	35.0	560	39.3	39.5
420	36.9	37.5	580	39.3	39.6
440	38.2	38.5	589	39.3	39.6
460	38.8	39.0	600	39.4	39.7
470	38.9	39.1	620	39.5	39.7
480	38.9	39.1	640	39.5	39.8
500	39.1	39.3	650	39.4	39.7
520	39.1	39.4	660	39.3	39.5
540	39.3	39.5	680	39.4	39.7
546	39.3	39.5	700	39.2	39.5

The values required by the Commission on Ore Mineralogy are given in bold.

**Fig. 3.** Reflectance data of maletoyvayamite.

Therefore, a synthetic $\text{Au}_3\text{Se}_4\text{Te}_6$ phase was prepared and subsequently used for a crystal structure analysis. The X-ray diffraction data obtained from the natural material (the largest grain of size 20–50 μm) were not sufficient to solve the crystal structure.

Synthetic $\text{Au}_3\text{Se}_4\text{Te}_6$ was prepared using the evacuated silica glass tube method in the Laboratory of Experimental Mineralogy of the Czech Geological Survey in Prague. Gold (99.95%; additionally, refined at the laboratory using a digestion–precipitation technique), tellurium (99.999%) and selenium (99.999%) were used as starting materials for the synthesis. The evacuated silica-glass tube with its charge was sealed and heated at 400°C. Three times during the experiment, after cooling by a cold-water bath, the charge was ground into powder in acetone using an agate mortar, and thoroughly mixed to homogenise. The pulverised charge was sealed in an evacuated silica-glass tube again and heated at 400°C for 4 months. Finally, the experimental product was quenched rapidly in a cold-water bath.

Chemical composition

The polished sections prepared from both the natural and experimental samples were also examined using an electron probe microanalyser (EPMA, CAMECA SX-100) equipped with wavelength dispersion spectrometers (WDS). Quantitative data and chemical analysis were obtained using 15 kV acceleration voltage and 10 nA beam current (diameter: 1–2 μm). Standards were pure

metals (Au and Te), Bi_2Se_3 (Se) and FeS_2 (S). No other elements with atomic numbers higher than 8 were detected. The EPMA results for maletoyvayamite, both natural and synthetic are given in Table 2. The empirical formula, calculated for the mean composition ($n = 16$; measured on nine different grains) on the basis of 13 atoms per formula unit (apfu) is $\text{Au}_{2.90}(\text{Se}_{3.52}\text{S}_{0.44})_{\Sigma 3.96}\text{Te}_{6.14}$ for natural maletoyvayamite, the ideal chemical formula is $\text{Au}_3\text{Se}_4\text{Te}_6$ which requires Au 35.34, Se 18.88, Te 45.78, total 100 wt.%.

X-ray crystallography

Single-crystal diffraction study of synthetic analogue $\text{Au}_3\text{Se}_4\text{Te}_6$

As the natural crystals of maletoyvayamite proved to be unsuitable for crystal structure analysis, the relevant structural investigations were performed on a synthetic analogue $\text{Au}_3\text{Se}_4\text{Te}_6$. Only a powder X-ray diffraction pattern of natural maletoyvayamite was collected (see below). Single-crystal X-ray studies on synthetic analogue $\text{Au}_3\text{Se}_4\text{Te}_6$ were carried out using a Rigaku SuperNova single-crystal diffractometer with Atlas S2 CCD detector and monochromatised $\text{MoK}\alpha$ radiation from the microfocuss X-ray tube. The crystal structure was solved from single-crystal data using the program *SHELXT* (Sheldrick, 2015), and subsequently refined by the full-matrix least-squares of the *JANA2006* program (Petříček *et al.*, 2014). All atoms were refined with anisotropic displacement parameters; $R_1 = 0.0375$ for 2042 unique reflections with $I > 3\sigma(I)$ and 119 refined parameters. Crystallographic details and details for the structure refinement can be found in Table 3, atom coordinates and displacement parameters in Table 4 and selected interatomic distances in Table 5. The crystallographic information files have been deposited with the Principal Editor of *Mineralogical Magazine* and are available as Supplementary material (see below).

Powder X-ray diffraction study of natural maletoyvayamite and its synthetic analogue $\text{Au}_3\text{Se}_4\text{Te}_6$

The micro-powder X-ray diffraction data on a natural crystal of maletoyvayamite were acquired using a Rigaku-Oxford Diffraction Supernova diffractometer equipped with an X-ray micro-source ($\text{MoK}\alpha$) and a 200K Dectris detector on a grain with an average radius of 0.04 mm. The sample-to-detector distance was 68 mm. The data were measured over 0–360° in φ with an exposure time of 60 s per frame. A complete list of observed d values and relative intensities is reported in Table 6. The refined unit-cell parameters are: $a = 8.901(2)$, $b = 9.0451(14)$, $c = 9.265(4)$ Å, $\alpha = 97.66(3)^\circ$, $\beta = 106.70(2)^\circ$, $\gamma = 101.399(14)^\circ$ and $V = 685.9(4)$ Å³.

The powder X-ray diffraction data of the synthetic material were collected using Bruker D8 Advance diffractometer equipped with LynxEye XE detector in Bragg–Brentano geometry and using $\text{CuK}\alpha$ radiation. The data were collected in the range from 6° to 110°2 θ with a step size of 0.015°2 θ . Considering the low symmetry of the maletoyvayamite and resulting strong degree of reflections overlap in powder diffraction patterns, the unit-cell parameters were calculated using the Rietveld method in the *Topas 5* program (Bruker AXS, 2014). The structure model obtained from single-crystal study (see above) was used as the starting structure model in a subsequent Rietveld refinement of synthetic $\text{Au}_3\text{Se}_4\text{Te}_6$. The refined parameters include those

Table 2. Chemical composition of maletoyvayamite (wt.%) and its synthetic analogue.

Natural maletoyvayamite					
Grain no.	Au	Se	S	Te	Total
Wt.%					
2_7	34.80	16.15	1.18	48.27	100.40
2_7	35.19	15.73	1.32	47.91	100.14
2_7	34.27	16.28	1.03	47.28	98.86
2_7	34.87	16.36	1.22	47.95	100.39
2_3	35.65	17.03	0.38	47.41	100.48
3_7	34.83	16.97	0.72	47.53	100.05
3_7	34.59	16.87	0.82	47.79	100.06
3_7	35.02	16.75	0.78	47.00	99.54
3_8	33.16	18.90	0.66	46.24	98.95
3_8	34.26	18.24	0.68	45.12	98.30
4_3	34.44	15.86	0.94	46.80	98.05
4_11	33.98	16.67	0.88	46.56	98.09
5_1	34.32	16.24	0.83	46.85	98.23
6_1	33.69	16.62	0.71	47.64	98.67
6_1	34.29	16.60	0.71	48.02	99.63
6_3	33.93	16.96	0.63	47.24	98.76
Average	34.46	16.76	0.84	47.23	99.29
σ	0.61	0.81	0.24	0.80	0.89
Apfu on the basis of 13 atoms					
	Au	Se	S	Te	S + Se
2_7	2.88	3.34	0.60	6.18	3.94
2_7	2.92	3.26	0.67	6.14	3.93
2_7	2.89	3.42	0.53	6.15	3.96
2_7	2.88	3.37	0.62	6.12	3.99
2_3	3.02	3.59	0.20	6.19	3.79
3_7	2.92	3.55	0.37	6.16	3.92
3_7	2.89	3.52	0.42	6.17	3.94
3_7	2.95	3.52	0.40	6.12	3.93
3_8	2.77	3.94	0.34	5.96	4.27
3_8	2.90	3.85	0.35	5.90	4.21
4_3	2.94	3.38	0.49	6.18	3.88
4_11	2.89	3.54	0.46	6.11	4.00
5_1	2.93	3.46	0.43	6.18	3.89
6_1	2.86	3.52	0.37	6.25	3.89
6_1	2.89	3.49	0.37	6.25	3.86
6_3	2.88	3.59	0.33	6.20	3.92
Average	2.90	3.52	0.44	6.14	3.96
Synthetic					
(<i>n</i> = 7)	Au	Se		Te	
Wt.%					
Average	34.67	19.74		45.72	
σ	0.36	0.14		0.2	
Apfu based on 13 atoms					
	2.90	4.16		5.94	

describing crystal size, preferred orientation along [010] and unit-cell parameters. No fractional coordinates and displacement parameters were refined. The refinement converged to the agreement factor R_{wp} 13.89% and yielded refined unit-cell parameters: $a = 8.9835(3)$, $b = 9.1129(2)$, $c = 9.3090(3)$ Å, $\alpha = 97.29(1)^\circ$, $\beta = 107.11(1)^\circ$, $\gamma = 101.73(1)^\circ$, and $V = 698.81(6)$ Å³.

A comparison of powder X-ray diffraction data between maletoyvayamite and its synthetic analogue is shown in Table 6. The obtained unit-cell parameters are compared in Table 7. The positions and intensities of diffractions from a fragment of natural material extracted from the polished sections match very well with the diffraction pattern of synthetic Au₃Se₄Te₆ and consequently demonstrates the structural identity between natural material and its synthetic analogue. The structural identity was

Table 3. Single-crystal data collection and structure-refinement details for synthetic Au₃Se₄Te₆.

Crystal data	
Structural formula	Au ₃ Se ₄ Te ₆
Crystal size (μm)	41 × 26 × 21
Crystal system, space group	<i>P</i> $\bar{1}$
Temperature (K)	297
<i>a</i> , <i>b</i> , <i>c</i> (Å)	8.9697(8), 9.1117(9), 9.3034(7)
α , β , γ (°)	97.346(7), 107.143(7), 101.671(8) ^o
<i>V</i>	697.1298(11) Å ³
<i>Z</i>	2
Density (for above formula) (g cm ⁻³)	7.967
Absorption coefficient (mm ⁻¹)	54.19
Data collection	
Diffractometer	Rigaku SuperNova with Atlas S2 CCD
X-ray radiation/power	MoK α ($\lambda = 0.71075$ Å)/40 kV, 30 mA
<i>F</i> (000)	1370
θ range	2.93 to 29.37 ^o
Index ranges	-11 ≤ <i>h</i> ≤ 9, -10 ≤ <i>k</i> ≤ 12, -12 ≤ <i>l</i> ≤ 12
Reflections collected/unique	4506/2670; $R_{int} = 0.020$
Reflections with $I > 3\sigma$	2042
Completeness to $\theta = 29.37^\circ$	79.00%
Refinement	
Refinement method	Full-matrix least-squares on F^2
Parameter/restraints/constraints	119/0/0
GoF	1.49
Final <i>R</i> indices [$I > 3\sigma$]	$R_1 = 0.0375$, $wR_1 = 0.0840$
<i>R</i> indices (all data)	$R_2 = 0.0552$, $wR_2 = 0.0899$
Weighting scheme, weights	Based on measured s.u.'s, $w = 1/(\sigma^2(I) + 0.0004I^2)$
Largest diff. peak/hole (e ⁻ Å ⁻³)	+2.94/-2.52

further supported by Raman spectroscopy (see below). A few discrepancies in positions of diffractions might be due to the slightly different compositions of natural maletoyvayamite and its synthetic analogue. The minor difference in intensities might be due to using different diffraction methods (PseudoGandolfi versus Bragg–Brentano), radiations (MoK α versus CuK α) and preferred orientation observed in the diffraction pattern from Bragg–Brentano geometry.

Structure description

The crystal structure of maletoyvayamite contains three Au, six Te and four Se atoms in the asymmetric unit (Fig. 4). The structure is relatively simple and resembles a molecular structure. The basic structural unit is a molecular cluster with [Au₆Se₈Te₁₂] composition and can be described as a distorted cube with Se atoms at vertices. Au atoms occupy centres of the faces of the cube and Te atoms are placed at the midpoints of Se–Se edges. Each unit cell contains one cluster. Au atoms show a square planar coordination by four Te atoms, as is typical for Au in *d*⁸ configuration. Whereas Au1 atom shows four Te at almost equal distances of 2.68 Å, Au2 and Au3 atoms show two shorter (2.68 Å) and slightly longer (2.75 Å) Te contacts. This tiny difference in Au–Te bonds causes the slight distortion of the [Au₆Se₈Te₁₂] clusters from the ideal cubic shape. Se atoms, forming corners of the [Au₆Se₈Te₁₂] clusters, show three short Te contacts at distances ranging from 2.641(2) to 2.951(2) Å. The distortion of the cluster is mirrored by the values of Au–Se–Au angles ranging from 84.74(6)^o to 88.56(6)^o instead of being 90^o for an ideal cube. The Se and Te atoms have acentric environments implying stereoactivity of lone electron pairs.

Table 4. Atom coordinates, anisotropic and equivalent displacement parameters (\AA^2) for synthetic $\text{Au}_3\text{Se}_4\text{Te}_6$.

Atom	x/a	y/b	z/c	U_{eq}	U^{11}	U^{22}	U^{33}	U^{12}	U^{13}	U^{23}
Au1	0.57821(8)	0.79878(7)	0.55869(7)	0.0159(2)	0.0147(3)	0.0199(3)	0.0131(3)	0.0044(3)	0.0044(3)	0.0032(3)
Au2	0.40703(8)	0.49520(8)	0.18605(7)	0.0176(2)	0.0158(4)	0.0157(3)	0.0212(3)	0.0039(3)	0.0067(3)	0.0025(3)
Au3	0.81147(8)	0.50400(7)	0.50172(7)	0.0168(2)	0.0185(3)	0.0156(3)	0.0143(3)	0.0033(3)	0.0034(3)	0.0023(3)
Te1	0.90033(15)	0.50433(14)	0.81158(13)	0.0198(4)	0.0173(6)	0.0249(6)	0.0174(5)	0.0053(5)	0.0057(4)	0.0048(5)
Te2	0.33769(15)	0.18930(13)	0.13753(12)	0.0200(4)	0.0283(7)	0.0153(6)	0.0137(5)	0.0028(5)	0.0056(5)	0.0014(5)
Te3	0.50052(15)	0.80129(13)	0.25781(12)	0.0211(4)	0.0290(7)	0.0165(6)	0.0163(5)	0.0042(5)	0.0061(5)	0.0040(5)
Te4	0.71589(14)	0.49782(13)	0.19084(12)	0.0206(4)	0.0184(6)	0.0265(7)	0.0177(6)	0.0066(5)	0.0066(5)	0.0045(5)
Te5	0.72393(14)	0.19795(13)	0.45472(13)	0.0212(4)	0.0177(6)	0.0163(6)	0.0301(6)	0.0057(5)	0.0085(5)	0.0032(5)
Te6	0.88417(13)	0.80990(13)	0.57515(13)	0.0201(4)	0.0144(6)	0.0156(6)	0.0287(6)	0.0012(4)	0.0075(5)	0.0020(5)
Se1	0.9915(2)	0.82223(19)	0.87686(18)	0.0173(6)	0.0141(8)	0.0174(9)	0.0144(8)	-0.0007(7)	0.0004(7)	-0.0003(7)
Se2	0.6321(2)	0.1827(2)	0.12504(18)	0.0184(6)	0.0213(9)	0.0193(9)	0.0156(8)	0.0072(7)	0.0076(7)	0.0004(7)
Se3	0.8290(2)	0.1884(2)	0.75238(19)	0.0199(6)	0.0224(10)	0.0191(9)	0.0188(8)	0.0094(7)	0.0038(7)	0.0069(7)
Se4	0.7948(2)	0.81898(19)	0.24778(18)	0.0181(6)	0.0172(9)	0.0167(9)	0.0188(8)	0.0003(7)	0.0060(7)	0.0042(7)

Table 5. Selected bond distances (\AA) for synthetic $\text{Au}_3\text{Se}_4\text{Te}_6$.

Au1–Te2	2.6832(13)	Au2–Te1	2.7644(17)	Au3–Te1	2.7546(14)
Au1–Te3	2.6823(14)	Au2–Te2	2.6778(15)	Au3–Te4	2.7532(13)
Au1–Te5	2.6824(16)	Au2–Te3	2.6786(15)	Au3–Te5	2.6803(14)
Au1–Te6	2.6835(15)	Au2–Te4	2.7528(16)	Au3–Te6	2.6788(14)
Au2–Te4	3.367(2)	Au3–Au3	3.410(1)		

The $[\text{Au}_6\text{Se}_8\text{Te}_{12}]$ clusters are linked in the $[100]$ direction (Fig. 5) via weak Se–Se (3.39 \AA) and Au–Au (3.41 \AA) interactions. The linkage in approximate $[010]$ and $[001]$ directions is achieved through weak Se–Se (3.37 \AA), Au–Te (3.36), Au–Se (3.69 \AA), Te–Te (3.69 \AA) and Te–Se (3.77 \AA) interactions. It is interesting to note that Au atoms form an octahedron within the

$[\text{Au}_6\text{Se}_8\text{Te}_{12}]$ cluster with Au–Au distances ranging from 3.79 to 3.95 \AA (Fig. 5). These distances are shorter than the Au–Au contacts between the $[\text{Au}_6\text{Se}_8\text{Te}_{12}]$ clusters (see above), however they indicate a certain degree of weak interactions.

The crystal structure of maletoyvayamite represents a unique structure type; no exact structural analogues among minerals are known. It is a molecular structure and hence it is structurally very different from the well-known gold tellurides (e.g. Bindi *et al.*, 2018 and references therein). The presence of molecular clusters in the maletoyvayamite structure resembles crystal structures of realgar, AsS, though that structure contains As_4S_4 molecules (Mullen and Nowacki, 1972) and hence is structurally very different from maletoyvayamite. The structure of sinnerite $[\text{Cu}_6\text{As}_4\text{S}_9]$ (Bindi *et al.*, 2013) is metrically close to maletoyvayamite, however it contains an As_4S_{12} molecular cluster composed

Table 6. Comparison of powder XRD patterns (d in \AA) of maletoyvayamite and its synthetic analogue $\text{Au}_3\text{Se}_4\text{Te}_6$.

Natural maletoyvayamite ^a		Synthetic $\text{Au}_3\text{Se}_4\text{Te}_6$ ^b		
l_{obs}	d_{obs}	l_{obs}	d_{obs}	hkl
25	8.650	10	8.7213	010, 001
		3	8.3049	100
		1	5.6218	011
5	4.331	2	4.3601	020, 002, $1\bar{2}0$, $20\bar{1}$
		2	4.2584	$0\bar{1}2$, $0\bar{2}1$
1	3.888	1	3.8526	$1\bar{2}\bar{1}$
1	3.724	1	3.6808	$20\bar{2}$, $21\bar{1}$, $12\bar{1}$
3	3.444	2	3.4287	$0\bar{2}2$, 210
		8	2.9630	$3\bar{1}1$, $0\bar{1}3$
		12	2.9346	$0\bar{1}3$, 112
100	2.911	100	2.9132	$0\bar{1}3$, $1\bar{3}1$, 030
		2	2.8544	$3\bar{1}0$, $2\bar{2}\bar{1}$
3	2.619	2	2.6241	$2\bar{3}\bar{1}$, $31\bar{1}$, 031, 013
3	2.284	2	2.2990	$3\bar{3}\bar{1}$, $11\bar{4}$, $0\bar{3}3$, $2\bar{3}2$, 131, $1\bar{4}0$, $20\bar{4}$
		5	2.2338	032, $3\bar{2}2$, $21\bar{4}$, 023
7	2.223	2	2.2212	133, $4\bar{1}\bar{1}$, $3\bar{2}\bar{1}$, $0\bar{4}1$, $3\bar{2}2$, 032, 023, $0\bar{1}4$
6	2.180	13	2.1847	040
		4	2.1315	$3\bar{1}2$, $0\bar{4}2$
3	2.072	5	2.0773	$3\bar{2}2$, $2\bar{4}\bar{1}$, $4\bar{2}2$, $3\bar{2}3$, 203, $30\bar{4}$, 400, $2\bar{2}4$, $14\bar{1}$
		4	1.9511	$3\bar{4}1$
8	1.930	13	1.9410	$13\bar{4}$, $0\bar{4}3$, 231 , $0\bar{3}4$, $41\bar{3}$, $4\bar{2}1$, $2\bar{4}2$
8	1.901	11	1.8852	$3\bar{3}\bar{1}$, 312, $1\bar{4}2$, 410, 213, $3\bar{4}1$, 321, $4\bar{3}2$, $3\bar{3}2$, $1\bar{4}3$, $14\bar{1}$
6	1.725	8	1.7485	240, 152, $4\bar{4}\bar{1}$, 050, 440, $50\bar{1}$
		1	1.4954	$6\bar{1}2$, $4\bar{3}3$
		2	1.4815	$0\bar{1}6$, 256, $6\bar{2}2$
		13	1.4569	060, $1\bar{1}6$, 262 , $26\bar{1}$

^aObtained by the pseudoGandolfi method, micro-source MoK α radiation.^bCollected in Bragg–Brentano geometry, CuK α radiation.

Table 7. Comparison between unit-cell parameters obtained by powder XRD performed on maletoyvayamite, and powder and single-crystal XRD on its synthetic analogue.

	Maletoyvayamite (powder XRD)	Synthetic analogue (single-crystal diffraction)	Synthetic analogue (powder XRD)
a (Å)	8.901(2)	8.9697(8)	8.9835(3)
b (Å)	9.0451(14)	9.1117(9)	9.1129(2)
c (Å)	9.265(4)	9.3034(7)	9.3090(3)
α (°)	97.66(3)	97.346(7)	97.29(1)
β (°)	106.70(2)	107.143(7)	107.11(1)
γ (°)	101.399(14)	101.671(8)	101.73(1)
V (Å ³)	698.9(4)	697.1298(11)	698.81(6)

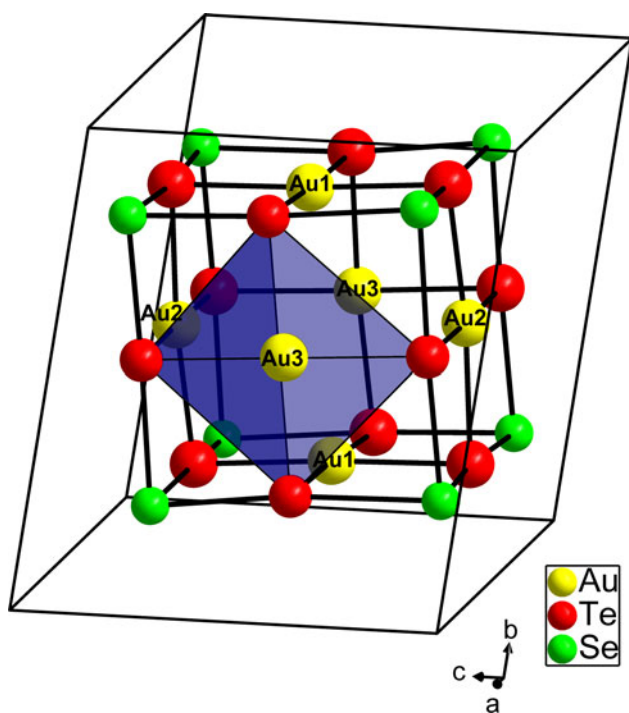


Fig. 4. Crystal structure of $\text{Au}_3\text{Se}_4\text{Te}_6$ showing the $[\text{Au}_6\text{Se}_8\text{Te}_{12}]$ cluster. The $[\text{AuTe}_4]$ square is emphasised (blue shading) for clarity.

of four AsS_3 coordination pyramids. The crystal structure of the chemically related synthetic phase α -AuSe can be described as packing of infinitely long AuSe molecules parallel to the b axis (Rabenau and Schulz, 1976). These molecules are connected by weak Au–Au (3.22 Å) and Se–Se (3.35–3.73 Å) interactions. However, a linear coordination of Au atoms observed in α -AuSe was not observed in the maletoyvayamite structure. Similar to the $[\text{Au}_6\text{Se}_8\text{Te}_{12}]$ unit is the $[\text{Re}_6\text{Se}_8(\text{OH})_6]$ cluster observed in the structure of the $\text{K}_4[\text{Re}_6\text{Se}_8(\text{OH})_6] \cdot 5\text{H}_2\text{O}$ synthetic phase (Brylev 2013), however it lacks the atoms positioned at the midpoints of edges of the Se_8 cube (i.e. Te atoms in maletoyvayamite).

Raman spectroscopy

Raman spectroscopy was applied to four grains of maletoyvayamite and compared with its synthetic analogue $\text{Au}_3\text{Se}_4\text{Te}_6$. The Raman spectra of natural and synthetic $\text{Au}_3\text{Se}_4\text{Te}_6$ are shown in Fig. 6.

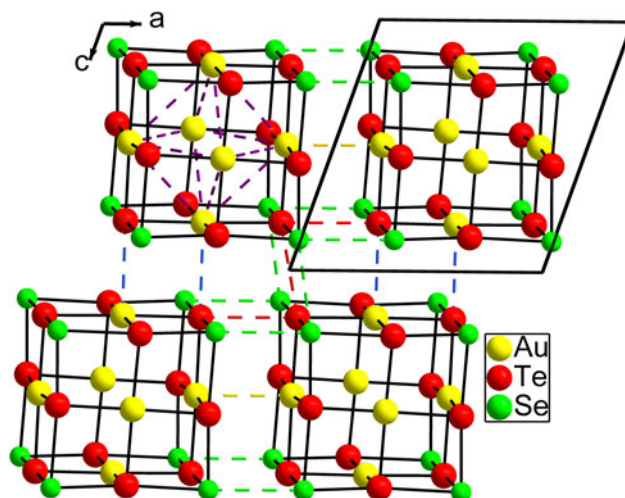


Fig. 5. System of weak bond interactions between $[\text{Au}_6\text{Se}_8\text{Te}_{12}]$ clusters in the crystal structure of $\text{Au}_3\text{Se}_4\text{Te}_6$. Green, yellow, red and blue dashed lines represent Se–Se, Au–Au, Te–Te and Au–Te weak interactions between clusters, respectively. Violet dashed lines indicate weak Au–Au interactions within in one of $[\text{Au}_6\text{Se}_8\text{Te}_{12}]$ cluster.

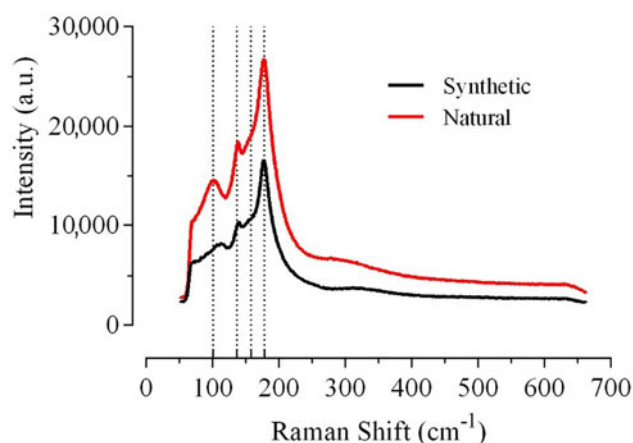


Fig. 6. Raman spectrum of maletoyvayamite in comparison with its synthetic analogue $\text{Au}_3\text{Se}_4\text{Te}_6$.

Raman spectra were obtained in back-reflecting geometry using an S&I MonoVista CRS+ Raman microspectrometer (spectrometer SP2750i, Princeton Instruments; grating 1800 gr./mm) equipped with a Peltier-cooled Andor iDus-416 CCD detector (size 2000×256 pixels, pixel size $15 \times 15 \mu\text{m}$) and Cobolt Samba 100 mW Nd–YAG laser source (nominal wavelength $\lambda = 532 \text{ nm}$) installed at the Czech Academy of Sciences, Institute of Geology, Prague, Czech Republic. Laser power on the sample was measured with a Coherent LaserCheck pencil-style power meter as 1.8 mW. An upright microscope Olympus BX-51 WI with a $100\times$ magnifying objective was used to direct the laser beam on the sample and to collect the Raman signal. An exposure time of 10 s with 25 accumulations and a single-frame correction for cosmic radiation was used to acquire the spectra. The wavelength scale was calibrated with an IntelliCal Hg–Ne–Ar lamp and Raman band positions were checked against those of silicon and polystyrene standards. The obtained Raman spectra of natural and synthetic $\text{Au}_3\text{Se}_4\text{Te}_6$ show four discernible absorption bands at the following values: 101, 137, 158 and 178 cm^{-1} (Fig. 6).

The Raman spectra of maletoyvayamite and its synthetic analogue $\text{Au}_3\text{Se}_4\text{Te}_6$ (Fig. 6) are identical and further supports the structural identity between synthetic and natural material.

Genetic implications

The Gaching ore occurrence of the Maletoyvayam deposit belongs to the HS (high sulfidation) type of epithermal deposits. Gold and Se-rich minerals are characteristic for this ore association that implies special conditions for their formation: an abundant source of Au and Se, and a strongly oxidising environment ($\text{pH} = 0\text{--}2$). Therefore, under these conditions Au selenides can be formed. Maletoyvayamite, $\text{Au}_3\text{Se}_4\text{Te}_6$, in intergrowths with Au–Ag alloys, Au tellurides, and other unnamed Au–Se–Te compounds are related to the main stage of ore mineralisation which is stable at 250°C in a $\log f_{\text{Se}_2}$ range of -12.4 and -5.7 (Tolstykh *et al.*, 2018). A further increase of f_{O_2} leads to oxidation of Au tellurides to Au, Ag(Sb, As, Te, S) oxides and formation of mustard gold (Tolstykh *et al.*, 2019b).

Supplementary material. To view supplementary material for this article, please visit <https://doi.org/10.1180/mgm.2019.81>.

Acknowledgements. The authors acknowledge Ritsuro Miyawaki, Chairman of the IMA–CNMNC and its members for helpful comments on the submitted data. The studies of minerals were carried out within the framework of the state assignment of the VS Sobolev Institute of Geology and Mineralogy of SB RAS. The authors would like to thank Vladimir Korolyuk and Mikhail Khlestov for assisting during analytical procedures, Luboš Vrtiška (National Museum in Prague) for reflectance measurements, Roman Skála (Institute of Geology AS CR, v.v.i.) for Raman measurements and Zuzana Korbellová (Institute of Geology AS CR, v.v.i.) for EPMA. This research was supported by the Grant Agency of the Czech Republic (project No. 18-15390S), by Russian Foundation for Basic Research (RFBR No. 19-05-00316) and by the Ministry of Education, Youth and Sports National sustainability program I of the Czech Republic (project No. LO1603). Additional support came from the Ministry of Education and Science of the Russian Federation (project no. 14.Y26.31.0018). The authors would like to thank Peter Leverett and one anonymous reviewer for the comments and the Principal Editor Stuart Mills.

References

- Bindi L., Nestola F. and Makovicky E. (2013) Sinnerite, $\text{Cu}_6\text{As}_4\text{S}_9$, from the lengenbach quarry, Binn Valley, Switzerland: Description and re-investigation of the crystal structure. *The Canadian Mineralogist*, **51**, 851–860.
- Bindi L., Paar W.H. and Lepore G.O. (2018) Montbrayite, $(\text{Au,Ag,Sb,Pb,Bi})_{23}(\text{Te,Sb,Pb,Bi})_{38}$, from the Robb-Montbray mine, Québec: Crystal structure and revision of the chemical formula. *The Canadian Mineralogist*, **56**, 129–142.
- Bruker AXS (2014) *TOPAS Software User Manual Version 4.2*. Karlsruhe, Germany.
- Brylev K.A. (2013) Novel crystal structures of potassium salts of chalcogeno cluster complexes $[\text{Re}_6\text{Q}_8(\text{OH})_6]^{4-}$ ($\text{Q} = \text{S}$ or Se), *Journal of Structural Chemistry*, **54**, 196–200.
- Goryachev N.A., Volkov A.V., Gamyarin G.N., Sidorov A.A., Savva N.E. and Okrugin V.M. (2010) Au–Ag mineralization of volcanic belts of the North-East of Asia. *Lithosphere*, **5**, 33–50 [in Russian].
- Kalinin K.B., Andreeva E.D. and Yablokova D.A. (2012) Textures and structures of Jubilee ore occurrence (Maletoyvayam ore field). Pp. 39–48 in: *Materials XI Regional youth scientific conference “The Natural Environment of Kamchatka”*. Petropavlovsk-Kamchatsky, Russia [in Russian].
- Melkomukov B.H., Razumny A.V., Litvinov A.P. and Lopatin W.B. (2010) New highly promising gold objects of Koryakiya. *Mining Bulletin of Kamchatka*, **14**, 70–74 [in Russian].
- Mullen D.J.E. and Nowacki W. (1972) Refinement of the crystal structures of realgar, AsS and orpiment, As_2S_3 . *Zeitschrift für Kristallographie*, **136**, 48–65.
- Okrugin B.M. (2003) New data on the age and genesis of epithermal deposits of transition zone continent-ocean (Pacific Northwest): Geodinamika, magmatism and metallogeny of continental margins of the North Pacific. Pp. 39–41 in: *Materials XII All-Union conference “Annual Meeting of the North-Eastern Branch of the WMO”*. Magadan, Russia [in Russian].
- Okrugin V.M., Andreeva E.D., Yablokova D.A., Okrugina A.M., Chubarov V.M. and Ananiev V.V. (2014) The new data on the ores of the Aginskoye gold-telluride deposit (Central Kamchatka). Pp. 335–341 in: *Materials conference “Volcanism and its Associated Processes”*. Petropavlovsk-Kamchatsky, Russia [in Russian].
- Petříček V., Dušek M. and Palatinus L. (2014) Crystallographic computing system JANA2006: General features. *Zeitschrift für Kristallographie*, **229**, 345–352.
- Rabenau A. and Schulz H. (1976) The crystal structure of α -AuSe and β -AuSe. *Journal of the Less-Common Metals*, **48**, 89–101.
- Sheldrick G.M. (2015) Crystal Structure refinement with SHELX. *Acta Crystallographica*, **C71**, 3–8.
- Tolstykh N., Vymazalová A., Petrova E. and Stenin N. (2017) The Gaching Au mineralization in the Maletoyvayam ore field, Kamchatka, Russia. Pp. 195–198 in: *Materials Mineral Resources to Discover*. Proceedings of the 14th Biennial SGA Meeting, 17–20 August 2017, Quebec City, Canada, Vol. 1.
- Tolstykh N., Vymazalová A., Tuhý M., and Shapovalova M. (2018) Conditions of Au–Se–Te mineralization in the Gaching ore occurrence (Maletoyvayam ore field), Kamchatka, Russia. *Mineralogical Magazine*, **82**, 649–674.
- Tolstykh N., Palyanova G., Bobrova O. and Sidorov E. (2019a) Mustard gold of the Gaching ore deposit (Maletoyvayam ore Field, Kamchatka, Russia). *Minerals*, **9**, 489, <https://doi.org/10.3390/min9080489>
- Tolstykh N., Tuhý M., Vymazalová A., Plášil J., Laufek F., Kasatkin A.V. and Nestola F. (2019b) Maletoyvayamite, IMA 2019-021. CNMNC Newsletter No. 50, *Mineralogical Magazine*, **83**, <https://doi.org/10.1180/mgm.2019.46>
- Tsukanov N.V. (2015) Tectono-stratigraphic terranes of Kamchatka active margins: Structure, composition and geodynamics. Pp. 97–103 in: *Materials of the Annual conference “Volcanism and Related Processes”*. Petropavlovsk-Kamchatsky, Kamchatka Krai, Russia [in Russian]